Slow dynamics of neuronal excitability under pulse stimulation

Daniel Soudry* and Ron Meir
Department of Electrical Engineering, the Laboratory for Network Biology Research, Technion 32000 , Haifa , Israel

Neurons fire irregularly on multiple timescales when stimulated with a periodic pulse train. This raises two questions: Does this irregularity imply significant intrinsic stochasticity? Can existing neuron models be readily extended to describe behavior at long timescales? We show here that for commonly studied neuronal models, dynamics is not chaotic and can only produce stable and periodic firing patterns. This is done by transforming the neuron model to an analytically tractable piecewise linear discrete map. Thus we answer "yes" and "no" to the above questions, respectively.

PACS numbers: 87.19.ll, 05.45.Jn, 87.85.dm, 87.19.lc

Biological systems are commonly affected by a large variety of processes, at many timescales. This is also true for excitable systems, such as neurons [1]. The generation of a neuronal Action Potential (AP - a stereotypically shaped voltage "spike" [2]) in response to stimulation is determined by the voltage-coupled interaction of the various ion channels populating the cell's membrane [3]. This interaction is slowly modulated over time by various slow processes [4], such as accumulating changes in the cell's ionic concentrations or slow inactivation of ion channels [3]. A common way to probe these slow changes in the neuronal excitability is to periodically stimulate the neuron with current pulses, while measuring various neuronal response features, such as firing rate or AP latency. In the recent work of [5] such a method was applied for a duration of days. They observed that the neuronal response changes in an irregular and non-stationary manner, with power law statistics [6], over the entire range of experimental timescales (from seconds to days). At first glance, this interesting result might seem trivial given the large range of timescales of the slow processes - it is not unreasonable to assume that such a complex dynamical system will exhibit irregular chaotic behavior over a large range of timescales. In fact, using a similar protocol at high frequencies, [7, 8] also observed irregular neuronal response, which was attributed to chaos. However, as we show in this letter, this is not the case at lower, physiological, stimulation frequencies (as were used in [5]), and in the context of the rather general and commonly used biophysical conductance based models (Eq. (1)-(2)). This was demonstrated by reducing these conductance based models, under periodic pulse stimulation, to an equivalent simplified model which is essentially a contracting piecewise linear map (Eqs. (5) or (6)). Such discontinuous maps appear in many systems [9]. Specifically, we were able to find analytic expressions for the neuronal response, rule out chaos and show that the neuron's steady state firing patterns are highly regular and periodic - corresponding to simple and stable limit cycles in the excitability state space. This entails that in [5] the neuronal response must be significantly affected by ion channel noise [3, 10] and additional biophysical processes which cannot be straightforwardly modeled as part of a conductance-based model. In a later, more extensive work, we will show how, by taking into account noise and such processes we can fully reproduce [5].

The full model Consider a generic conductance based-model for an excitable point neuron

$$\dot{x}_j = f_j(\mathbf{x}, \mathbf{s}, I(t)) \quad , j = 1, .., m \tag{1}$$

$$\dot{s}_i = \epsilon h_i(\mathbf{x}, s_i) \quad , i = 1, ..., n \tag{2}$$

with bounded **fast** $\mathbf{x} \triangleq (x_1, .., x_m)$ and **slow** $\mathbf{s} \triangleq (s_1, .., s_n)$ variables, receiving periodic current pulse stimulation $I(t) = I_0 \sum_k \delta(t - kT)$. Assume that $\epsilon = 0$ for now, so $\mathbf{s}$ remains constant. Since (1) describes an **"excitable"** neuron, after each stimulation pulse, a brief response in $\mathbf{x}$ follows which quickly relaxes back to steady state, within time $\tau_{\mathbf{x}}$ (Fig. (1)a). For certain values of initial conditions and I_0, we get a stereotypical "weak" response in $\mathbf{x}$, for other values we get a stereotypical "strong" response (an AP), while only for a very small set of values do we get an "intermediate" response. Next we examine the case $\epsilon > 0$. For simplicity we assume, as is commonly done [4], that $h_i(\mathbf{x}, s_i)$ are linear,

$$h_i(\mathbf{x}, s_i) = \delta_i(\mathbf{x})(1 - s_i) - \gamma_i(\mathbf{x}) s_i , \tag{3}$$

where δ_i and γ_i are rate functions of $O(1)$ magnitude. Note that this paper's main results will also hold for general monotonic $h_i(\mathbf{x}, s_i)$. Moreover, in neurons under pulse stimulation, the linear form of (3) is actually quite general - since [11] showed how in this case Eq. (3) well approximates the dynamics of an ion channel with power law memory - allowing for an infinite number of states and timescales. Finally, we make the **timescale separation assumption**

$$\tau_{\mathbf{x}} \ll T \ll \tau_{\mathbf{s}} , \tag{4}$$

where $\tau_{\mathbf{s}} \approx \epsilon^{-1}$, relevant for stimulation protocols at physiological frequencies, as in [5] (see also Fig. (1)a). For concreteness, we illustrate the results with an experimentally fitted Hodgkin Huxley (HH) model [2] where $\mathbf{x} = (V, m, n, h)$ (voltage and gating variables), with the addition of a single slow gating variable s, representing slow sodium inactivation [12]. We refer to this model as the HHS model (parameters in supplement [13]).

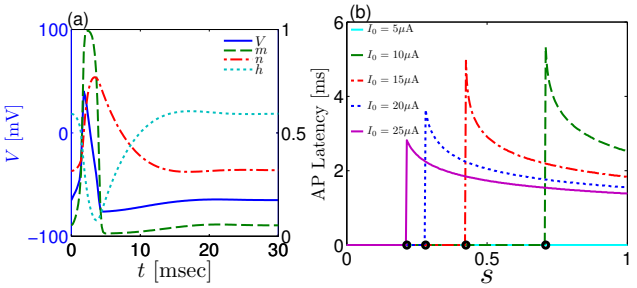

FIG. 1: **(a)** Relaxation of the HH model variables $\mathbf{x} = (V, m, n, h)$ to steady state after an AP ($I_0 = 15\,\mu$A). Relaxation is even faster if no AP is produced. The experiment of [5] was performed at $T \geq 20$ ms, for which $\tau_{\mathbf{x}} \ll T$. **(b)** AP latency, $L(s)$, in the HHS model, for different values of I_0. Firing thresholds $\theta \triangleq \{s|E(s) = 0\}$ are marked by black circles for each I_0. When no AP occurred, $L \triangleq 0$.

The simplified model The timescale separation assumption (4) allows us to replace the full model with a simpler, approximate model. Since $\tau_{\mathbf{x}} \ll T$ (Fig. 1a) only $\mathbf{s}$ retains memory of past stimulations. Therefore, to determine the neuronal behavior, it is only necessary to consider the dynamics of $\mathbf{s}$ and how it affects the system's response. We summarize the resulting model by four rules (derived below):
(1) At each stimulation an AP is produced if and only if $E(\mathbf{s}) > 0$, where E is the neuron's "excitability". In the 1D case $E(s) = s - \theta$ (Fig. 1b), while for several 2D neuron models we found a linear $E(\mathbf{s})$ [13].
(2) AP features, such as latency or maximum amplitude can be numerically calculated as functions of $\mathbf{s}$ (Fig. 1b).
(3) The change in $\mathbf{s}$ between consecutive stimulations is

$$\Delta s_i = \epsilon T \begin{cases} \delta_+^i (1 - s_i) - \gamma_+^i s_i & \text{, if } \mathbf{s} \in E_+ \\ \delta_-^i (1 - s_i) - \gamma_-^i s_i & \text{, if } \mathbf{s} \in E_- \end{cases}, \quad (5)$$

where $E_+ \triangleq \{\mathbf{s}|E(\mathbf{s}) > 0\}$ and $E_- \triangleq \{\mathbf{s}|E(\mathbf{s}) \leq 0\}$.
(4) $\gamma_\pm^i$ and $\delta_\pm^i$ all change linearly with $f_{\text{in}} \triangleq T^{-1}$.

In the context of this simplified model, the dynamics of the neuron are completely described by the dynamics of $\mathbf{s}$, which are determined by Eq. (5). These dynamics can be expressed as a piecewise linear recursive map $\mathbf{s}_{k+1} = \mathbf{g}(\mathbf{s}_k)$, where $\mathbf{s}_k$ is $\mathbf{s}$ at the time of the k-th stimulation, and

$$\mathbf{g}(\mathbf{s}) \triangleq A^{\pm}\left(\mathbf{s} - \mathbf{s}_\infty^{\pm}\right), \text{ if } \mathbf{s} \in E_\pm, \quad (6)$$

where both $A^\pm$ are diagonal and have eigenvalues inside the unit circle. This mapping is contracting everywhere except perhaps directly at the threshold - so chaos is ruled out. Specifically, any attractor $\mathcal{A}$ must be stable, with a possible exception in the case where $\|\mathcal{A} - \Theta\| = 0$, where $\Theta \triangleq \{\mathbf{s}|E(\mathbf{s}) = 0\}$. In the 1D case [14] proved that for almost all parameter values a unique (finite) limit cycle exists, and that it is globally stable - even if it contains θ. Similarly proving that the attractor is a globally stable limit cycle for the n-dimensional case might be hard - since [15] showed that determining global stability for general piecewise affine maps is undecidable. Simulations in the present setting indicated that we can get at most simple limit cycles [13], so we turned to explain this using more approximate methods. However, we first derive the simplified model in next section.

Simplified model derivation Rule 1 and 2 are straightforward. However, rules 3 and 4 require justification. Using Eq. (2) we write

$$\begin{aligned} \Delta s_i(t) &\triangleq \epsilon \int_t^{t+T} h_i(\mathbf{x}(u), s_i(u))\, du \\ &= \epsilon T\left[\bar{\delta}_i(t)(1 - s_i(t)) - \bar{\gamma}_i(t)\, s_i(t)\right] + O\left((\epsilon T)^2\right), \end{aligned} \quad (7)$$

where we have used the following notation for a time-averaged quantity

$$\bar{z}(t) \triangleq \frac{1}{T}\int_t^{t+T} z(\mathbf{x}(u))\, du\,. \quad (8)$$

We neglect the $O\left((\epsilon T)^2\right)$ correction term, since $\epsilon T \ll 1$. Since the value of $\mathbf{s}(t)$ determines the $\mathbf{x}$ dynamics in the interval $[t, t+T]$, it also determines $\bar{\gamma}_i(t)$ and $\bar{\delta}_i(t)$. Thus, slightly abusing notation, we write $\bar{\gamma}_i(\mathbf{s}(t))$ and $\bar{\delta}_i(\mathbf{s}(t))$ instead of $\bar{\gamma}_i(t)$ and $\bar{\delta}_i(t)$, respectively. Since the condition $\mathbf{s}(t) \in E_\pm$ determines whether or not an AP is generated, we expect that generally the sharpest changes in the values of $\bar{\gamma}_i(\mathbf{s})$ and $\bar{\delta}_i(\mathbf{s})$ occur near the threshold Θ. As can be seen in Fig. 2b, in the HHS case we indeed get a such a result. Following this reasoning, we make the assumption that the rates may be approximated as step functions with discontinuity on Θ

$$\bar{\gamma}_i(\mathbf{s}) = \gamma_\pm^i\,, \text{ if } \mathbf{s} \in E_\pm\,;\ \bar{\delta}_i(\mathbf{s}) = \delta_\pm^i\,, \text{ if } \mathbf{s} \in E_\pm. \quad (9)$$

The interpretation of this assumption is that the rates are insensitive to the $\mathbf{s}$ induced changes the AP shape and the steady state of $\mathbf{x}$. Together with Eq. (7), Eq. (9) gives Eq. (5).

Finally, to explain rule 4, we express the $[t, t+T]$ integral in (8) as the sum of two integrals on $[t, t+\tau_{\mathbf{x}}]$ and $[t+\tau_{\mathbf{x}}, t+T]$, and find that $\gamma_\pm^i$ and $\delta_\pm^i$ are all linear in f_{in}, since most of the response in $\mathbf{x}(t)$ after an AP is confined to $[t, t+\tau_{\mathbf{x}}]$ (see Fig. 2a).

Transient Phase We now return to the analysis of the simplified model. In Eq. (5) each s_i is coupled to the others only through the threshold. Therefore, if $\mathbf{s}(0)$ is far from Θ, each s_i will change independently forever, or until $\mathbf{s}(t)$ reach Θ. Until this happens it is perhaps more intuitive to describe the dynamics by the coarse-grained continuous-time version of Eq. (5)

$$\dot{s}_i(t) = -\epsilon\gamma_\pm^i s_i(t) + \epsilon\delta_\pm^i(1 - s_i(t))\,, \text{ if } \mathbf{s}(t) \in E_\pm. \quad (10)$$

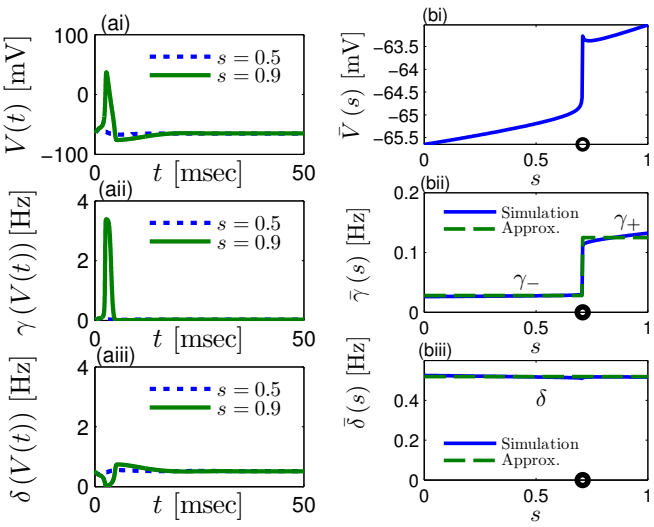

FIG. 2: Average rates in the HHS model, where the rates are functions of V. **(a)** dynamics of (i) voltage $V(t)$ (ii) $\gamma(V(t))$ and $(iii)\delta(V(t))$ after a stimulation pulse for two values of s. For $s = 0.5$ no AP occurred, while for $s = 0.9$ an AP was generated. Notice how $\gamma(V(t))$ is very different in each case, while $\delta(V(t))$ is approximately constant. **(b)** We derived $(i)\bar{V}(s)$ (ii) $\bar{\gamma}(s)$ and (iii) $\bar{\delta}(s)$ using Eq. (8), by simulations as in (a), for many values of s. Firing threshold θ is marked by a black circle. Notice that $\bar{\gamma}(s)$ changes significantly more than $\bar{\delta}(s)$, especially near to θ, and that $\bar{\gamma}(s)$ is approximated as a $\gamma_\pm$-valued step function as in Eq. (9) while $\bar{\delta}(s) \equiv \delta$, a constant. $I_0 = 10\,\mu$A and $T = 50$ ms.

The solution, for each case, is given by (see Fig. (3)aii)

$$s_i(t) = s^{\pm}_{\infty,i} + \left(s_i(0) - s^{\pm}_{\infty,i}\right) e^{-t/\tau^{\pm}_i}, \text{ if } \mathbf{s}(t) \in E_{\pm}, \quad (11)$$

where $\tau^{\pm}_i \triangleq \epsilon^{-1}\left(\delta^{\pm}_i + \gamma^{\pm}_i\right)^{-1}$, $s^{\pm}_{\infty,i} \triangleq \delta^{\pm}_i / \left(\delta^{\pm}_i + \gamma^{\pm}_i\right)$. In the HHS (1D) case, this gives, together with rule 4, a linear relation of the latency transient rate in f_{in}, as measured in [5].

Steady State Eventually $\mathbf{s}(t)$ arrives at some stable steady state behavior. There are several different possible steady states modes, depending on $\mathbf{s}^{\pm}_{\infty}$, which are affected by the amplitude and frequency of stimulation. These could be found by the following self-consistency arguments.

(i) Stable: If $E(\mathbf{s}^{+}_{\infty}) > 0$, $E(\mathbf{s}^{-}_{\infty}) > 0$ then $\mathbf{s}(t)$ stabilizes at $\mathbf{s}^{+}_{\infty}$, so APs are generated after each stimulation.

(ii) Unresponsive: If $E(\mathbf{s}^{+}_{\infty}) < 0$, $E(\mathbf{s}^{-}_{\infty}) < 0$ then $\mathbf{s}(t)$ stabilizes at $\mathbf{s}^{-}_{\infty}$, so no APs occur.

(iii) Bi-stable: If $E(\mathbf{s}^{+}_{\infty}) > 0$, $E(\mathbf{s}^{-}_{\infty}) < 0$ then, depending on the initial condition, $\mathbf{s}(t)$ stabilizes either on $\mathbf{s}^{+}_{\infty}$ (as in *(i)*) or on $\mathbf{s}^{-}_{\infty}$ (as in *(ii)*). This type of behavior is exhibited only in cases when the neuron becomes more excitable after an AP ("positive feedback").

(iv) Intermittent: If $E(\mathbf{s}^{+}_{\infty}) < 0$, $E(\mathbf{s}^{-}_{\infty}) > 0$ then steady state is always "on the other side" of the threshold Θ. Because of that, $\mathbf{s}(t)$ will stabilize near Θ. In this regime, small changes in $\mathbf{s}$ dominate the behavior of the neuron: the neuron alternates between an "on" state, in which $E(\mathbf{s}) > 0$ and the neuron can generate an AP at each stimulation, and an "off" state in which $E(\mathbf{s}) \leq 0$ and the neuron does not generate any AP (see Fig. (3)ai). This type of behavior is exhibited only in cases when the neuron becomes less excitable after an AP ("negative feedback").

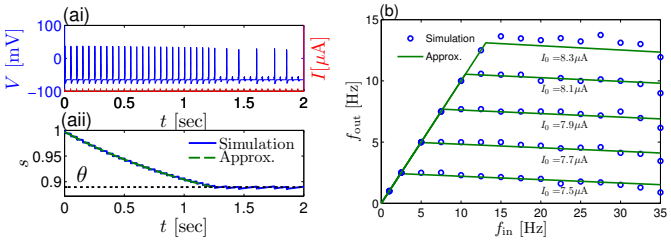

FIG. 3: Full HHS simulation under pulse stimulation. **(ai)** Pulses ($I_0 = 10\,\mu$A) generate APs every period, until an intermittent mode is reached, and AP failures ensue. **(aii)** s transiently decreases as predicted by Eq. (11), until θ is reached, then s stabilizes near θ during the intermittent mode. **(b)** Intermittent mode firing rate: comparison between full HHS simulation and the linear solution of Eq. (12).

Since $\mathbf{s}^{\pm}_{\infty}$ change with f_{in}, the steady state depends on f_{in}, as in [5]. For example, in the HHS case we get three possible types, depending on two critical frequencies f^1_{in} and f^2_{in} (both have closed form expressions). If $f_{\text{in}} < f^1_{\text{in}}$, the steady state is the stable mode, if $f^1_{\text{in}} < f_{\text{in}} < f^2_{\text{in}}$, it is the intermittent mode, and if $f_{\text{in}} > f^2_{\text{in}}$ it is the unresponsive mode.

Intermittent Mode Firing Rate We denote by p the time-averaged probability of generating an AP at steady state. The only case where $p \neq 0, 1$ is the intermittent mode. In this mode $\mathbf{s}$ is near the threshold Θ, so p can be derived by solving the self-consistent equation

$$E(\mathbf{s}_{\infty}(p)) = 0, \quad (12)$$

where $\gamma^i(p) \triangleq \gamma^i_+ p + \gamma^i_-(1-p)$, similarly $\delta^i(p)$, and $s^i_{\infty}(p) \triangleq \delta^i(p) / \left(\delta^i(p) + \gamma^i(p)\right)$. For example, in the HHS case we derive a simple linear relation for $\bar{f}_{\text{out}}(f_{\text{in}}) \triangleq p f_{\text{in}}$, as in [5]. This equation faithfully describes the firing rate of the full HHS model as long as the timescale separation assumption holds true (Fig. 3b).

Intermittent mode firing patterns Assume we solved (12) for p. Under the assumption that in steady state $\mathbf{s}$ remains near $\mathbf{s}_{\infty}(p)$, from Eqs. (5) and (9) we get that $\Delta s_i(\mathbf{s}) \approx \Delta s^{\pm}_i$, if $\mathbf{s} \in E_{\pm}$, where

$$\Delta s^{\pm}_i \triangleq \epsilon T \left(\delta^i_{\pm}\left(1 - s^i_{\infty}(p)\right) - \gamma^i_{\pm} s^i_{\infty}(p)\right) \quad (13)$$

It is easy to show that $\forall i : \Delta s^{+}_i / \Delta s^{-}_i = 1 - p^{-1} < 0$. This means that $\Delta\mathbf{s}^{+}$ has the opposite direction to $\Delta\mathbf{s}^{-}$ - so $\mathbf{s}$ remains on a simple one-dimensional limit cycle.

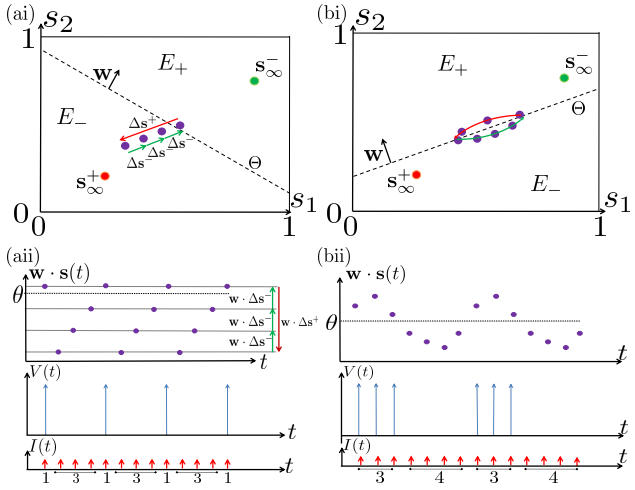

FIG. 4: Schematic state space dynamics of $\mathbf{s}$ and firing patterns in the intermittent mode in a 2D system. **(ai)** For $\mathbf{w}\cdot\Delta\mathbf{s}^+ < 0$ we get, from Eq. (13), a 1D limit cycle with $\Delta\mathbf{s}^+ = -q\Delta\mathbf{s}^-$ (here $q = 3$). **(aii)** Resulting $1 : q$ (AP:No AP) firing patterns for 1D limit cycle. **(bi)** 2D limit cycle when $\mathbf{w}\cdot\Delta\mathbf{s}^+ > 0$. **(bii)** Resulting $m : n$ firing patterns ("bursts") for 2D limit cycle. See [13] for simulations.

If $q \triangleq p^{-1} - 1 \geq 1$, the AP firing pattern is simple and repetitive: one period with an AP, followed by either $\lfloor q \rfloor$ or $\lfloor q \rfloor + 1$ periods in which no AP occurred (Fig. 4a). If instead $q < 1$, the firing pattern is different, yet still simple and repetitive: one period in which no AP occurred, followed by either $\lfloor q^{-1} \rfloor$ or $\lfloor q^{-1} \rfloor + 1$ periods with APs.

However, in some cases, this simple description cannot be true. Assume that $\mathbf{s}$ remains near $\mathbf{s}_\infty(p)$. In this case we can linearize $E(\mathbf{s}) \approx \mathbf{w}\cdot\mathbf{s} - \theta$. Without loss of generality, assume that $q > 1$ and $\theta < \mathbf{w}\cdot\mathbf{s}_k$, so an AP was produced at period k. In this case, according to the above description, $\mathbf{s}_{k+1} \approx \mathbf{s}_k + \Delta\mathbf{s}^+$ and in period $(k+1)$ no AP will be produced - so $\theta \geq \mathbf{w}\cdot(\mathbf{s}_k + \Delta\mathbf{s}^+)$. But this necessarily means that $0 > \mathbf{w}\cdot\Delta\mathbf{s}^+$. If this condition is not fulfilled (or, equivalently, $0 < \mathbf{w}\cdot\Delta\mathbf{s}^-$), then the above description of the firing patterns cannot be correct. Instead, $\mathbf{s}$ still revolves around $\mathbf{s}_\infty(p)$, but now in a higher-dimensional limit cycle (not 1D). In this case, the firing patterns are somewhat more general than before: $\mathbf{s}$ may remain on one side of the threshold Θ for several cycles, so the neuron can fire continuously for several periods, and then be silent for several more (Fig. 4b). The mechanism behind the firing patterns in the case $\mathbf{w}\cdot\Delta\mathbf{s}^+ > 0$ is similar to the mechanism behind "slow wave" bursts, that can occur in the standard current step stimulation of neurons [4], and includes at least two opposing types of gating variables ("positive feedback" + "negative feedback").

Discussion In summary, we have developed a method to simplify conductance-based models (Eq. (1)-(2)) under periodic pulse stimulation, given the timescale separation assumption. The simplified model is analytically solvable, leading to closed form expressions for the transient behavior, Eq. (11), a steady state firing rate input output relation, Eq. (12), and the firing patterns (Fig. 4). We ruled out chaos and showed that steady states solutions correspond to stable and simple limit cycles - and so the firing patterns the neuron model can produce are regular, periodic, stable and rather simple, in contrast to the results of [5]. Simulations indicate that this result is quite generic, and does not crucially depends on assumption (4). This result, in addition to the near-threshold behavior of the system, and the slow kinetics of the $\mathbf{s}$ gating variables, indicate that ion channel stochasticity [3, 10] is likely to be the generator of the observed irregularity. Even with addition of such noise, one can show that Eq. (12) does not allow firing rate to fluctuate much, and results in simple stationary statistics. Therefore, any number of slow processes of the form (2) is not sufficient to reproduce the non-stationary behavior observed in [5]. This implies that in order to correctly model a neuron at long timescales, existing models must be revised or extended. Such extensions will be addressed in future work.

Acknowledgments The authors are grateful to E. Braun, N. Brenner, Y. Elhanati, A. Gal, Y. Kafri, S. Marom and A. Wallach for many insightful discussions. R.M. was partially supported by the Technion fund for promotion of research and by the Ollendorf foundation.

* Corresponding author: daniel.soudry@gmail.com

[1] S. Marom, Prog. Neurobiol. **90**, 16 (2010).
[2] A. L. Hodgkin and A. F. Huxley, J. Physiol. **117**, 500 (1952).
[3] B. Hille *Ion channels of excitable membranes* (Sinauer Assoc., Sunderland, MA, 2001), 3rd ed.
[4] E. M. Izhikevich, *Dynamical systems in neuroscience* (MIT Press, Cambridge, MA, 2006).
[5] A. Gal *et al.*, J. Neurosci. **30**, 16332 (2010).
[6] G. Rangarajan and M. Ding, Phys. Rev. E **61**, 4991 (2000).
[7] G. Matsumoto *et al.*, Phys. Lett. A **123**, 162 (1987).
[8] D. Kaplan *et al.* , Phys. Rev. Lett. **76**, 4074 (1996).
[9] M. Di Bernardo, *Piecewise-smooth dynamical systems: theory and applications* (Springer Verlag, London, 2008).
[10] J. H. Goldwyn, N. S. Imennov, M. Famulare, and E. Shea-brown, Phys. Rev. E, in press (2011).
[11] D. Soudry and R. Meir, Front. Comput. Neurosci. **4** (2010).
[12] W. Chandler and H. Meves, J. Physiol. **211**, 707 (1970).
[13] See supplement.
[14] J. Keener, Trans. Amer. Math. Soc. **261**, 589 (1980).
[15] V. Blondel *et al.*, Theoret. Comput. Sci **255**, 687 (1999).

Slow dynamics of neuronal excitability under pulse stimulation - Supplementary Material

Daniel Soudry, Ron Meir
Department of Electrical Engineering,
the Laboratory for Network Biology Research,
Technion 32000 , Haifa , Israel

April 11, 2011

Simulations Details

In all simulations we used square pulses with duration $t_0 = 1$ ms and amplitude I_0 as stimulation pulses.

HH Model The classical Hodgkin-Huxley (HH) conductance-based model [4]:

$$\begin{aligned} C\dot{V} &= I_{Na} + I_K + I_L + I(t) = \bar{g}_{Na} m^3 h (E_{Na} - V) + \bar{g}_K n^4 (E_K - V) + \bar{g}_L (E_L - V) + I(t) \\ \dot{m} &= \alpha_m(V)(1-m) - \beta_m(V) m \\ \dot{n} &= \alpha_n(V)(1-n) - \beta_n(V) n \\ \dot{h} &= \alpha_h(V)(1-h) - \beta_h(V) h \end{aligned}$$

where $I(t)$ is the input current, V is the membrane's voltage and m, n and h are the gating variables of the channels. The parameters were given their standard values (as in [4, 2]):

$$C_m = 1\ \mu\mathrm{F}/cm^2, V_{Na} = 50\ \mathrm{mV}, V_K = -77\ \mathrm{mV}, V_L = -54\ \mathrm{mV},$$

$$\bar{g}_{Na} = 120\ (k\Omega \cdot cm^2)^{-1}, \bar{g}_K = 36\ (k\Omega \cdot cm^2)^{-1}, g_L = 0.3\ (k\Omega \cdot cm^2)^{-1},$$

and we used the standard rate functions

$$\begin{aligned} \alpha_n(V) &= \tfrac{0.01(V+55)}{1-e^{-0.1\cdot(V+55)}}\ \mathrm{kHz}, & \beta_n(V) &= 0.125 \cdot e^{(-(V+65)/80)}\ \mathrm{kHz}, \\ \alpha_m(V) &= \tfrac{0.1(V+40)}{1-e^{-0.1\cdot(V+40)}}\ \mathrm{kHz}, & \beta_m(V) &= 4 \cdot e^{(-(V+65)/18)}\ \mathrm{kHz}, \\ \alpha_h(V) &= 0.07 \cdot e^{(-(V+65)/20)}\ \mathrm{kHz}, & \beta_h(V) &= \left(e^{-0.1\cdot(V+35)} + 1\right)^{-1}\ \mathrm{kHz}, \end{aligned}$$

where in all the rate functions V is used in mV units.

HHS Model We incorporate slow sodium inactivation into the HH model as in [1, 5, 3], by introducing s, a new slow inactivation gate variable, into the sodium current

$$I_{Na} = \bar{g}_{Na} m^3 h s (E_{Na} - V)\ ,$$

where, as in [3], s have first order kinetics,

$$\dot{s} = \delta(V)(1-s) - \gamma(V) s\,,$$

with

$$\delta(V) = e^{-(V+85)/30}\ \mathrm{Hz}, \gamma(V) = 34 \cdot (e^{-0.1\cdot(V+17)} + 1)^{-1}\ \mathrm{Hz}.$$

HHSAP Model We now take the HHS model, rename $\{s, \gamma, \delta\} \rightarrow \{s_1, \gamma_1, \delta_1\}$, and add a slowly **A**ctivating **P**otassium current with M-current kinetics [6], so the total potassium current should now be

$$I_K = \bar{g}_K n^4 (E_K - V) + \bar{g}_K n^4 s_2 (E_K - V) .$$

with

$$\dot{s}_2 = \delta_2 (V) (1 - s) - \gamma_2 (V) s ,$$

where

$$\delta_2 (V) = \frac{3.3e^{(V+35)/40} + e^{-(V+35)/20)}}{1 + e^{-(V+35)/10}} \text{ Hz}, \; \gamma_2 (V) = \frac{3.3e^{3(V+35)/40} + e^{-3(V+35)/20)}}{1 + e^{-(V+35)/10}} \text{ Hz}$$

In Fig. 1 we see that for this model we get a linear threshold, and also step-like rate functions, as we discuss in the main text. Since this model contains only "negative feedback", we get only 1D limit cycle at steady state, and $1 : q$ or $q : 1$ firing patterns (as explained in main text, and as we see in Fig. 2).

HHSIP Model We now take the HHSPA, switch the potassium rates $\{\gamma_2, \delta_2\} \rightarrow \{\delta_2, \gamma_2\}$- so now potassium is **I**nactivating ("positive feedback") instead of **A**ctivating ("negative feedback"), and also make slow sodium inactivation somewhat slower $\{\gamma_1, \delta_1\} \rightarrow \{0.5\gamma_1, 0.5\delta_1\}$. These changes allow us to break the condition $\mathbf{w} \cdot \Delta s^+ < 0$ and get $m : n$ "bursts" (as explained in main text, and as we see in Fig. 3).

A: $I_0 = 10\ \mu$A

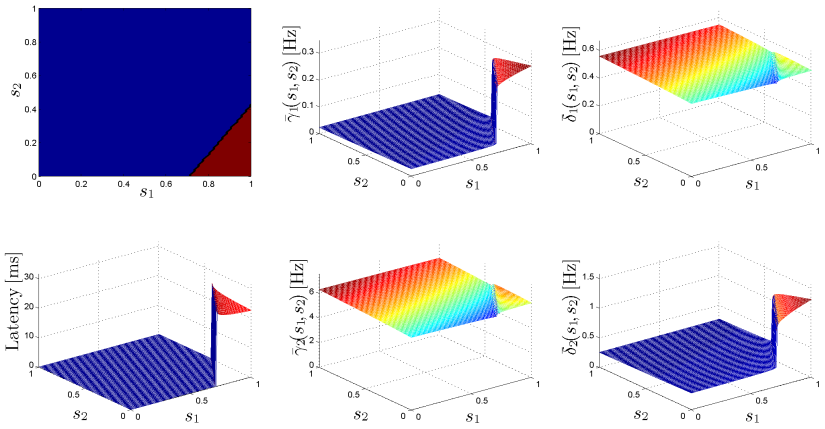

B: $I_0 = 14\ \mu$A

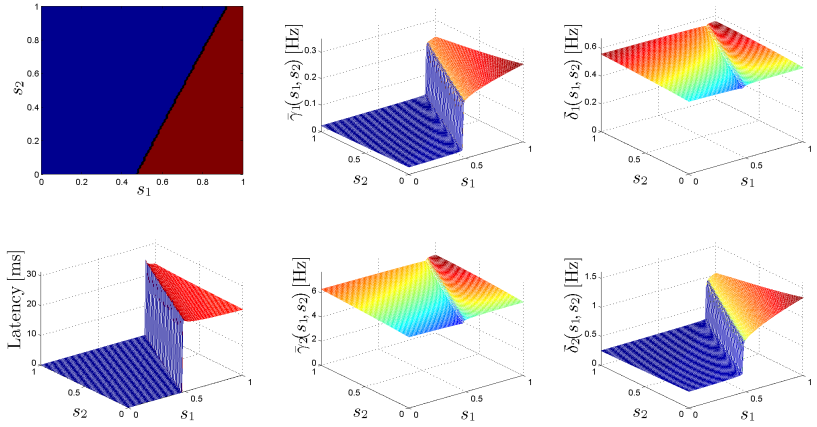

C: $I_0 = 20\ \mu$A

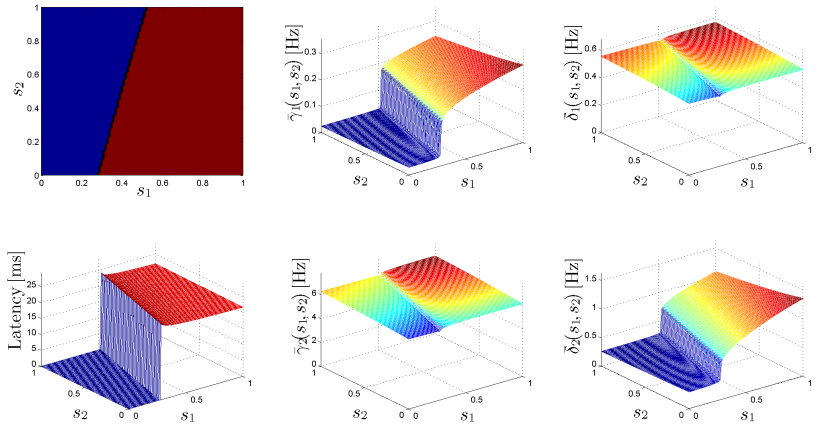

Figure 1: **A,B** and **C** show, for three different current amplitudes, the two-dimensional thresholds (*top left)*, latency functions (*bottom left)* and average rates for the HHSAP model (the other four graphs, showing respectively in a clockwise manner $\bar{\gamma}_1(\mathbf{s}), \bar{\gamma}_2(\mathbf{s}), \bar{\delta}_1(\mathbf{s})$ and $\bar{\delta}_2(\mathbf{s})$). We used here $T = 50$ ms. Notice that as before the sodium inactivation rate $\bar{\gamma}_1(\mathbf{s})$ has a step-like shape, while the sodium recovery rate $\bar{\delta}_1(\mathbf{s})$ is approximately constant. The situation is reversed for the potassium rates: the activation rate $\bar{\delta}_2(\mathbf{s})$ has the step-like shape, while the deactivation rate $\bar{\gamma}_2(\mathbf{s})$ is approximately constant.

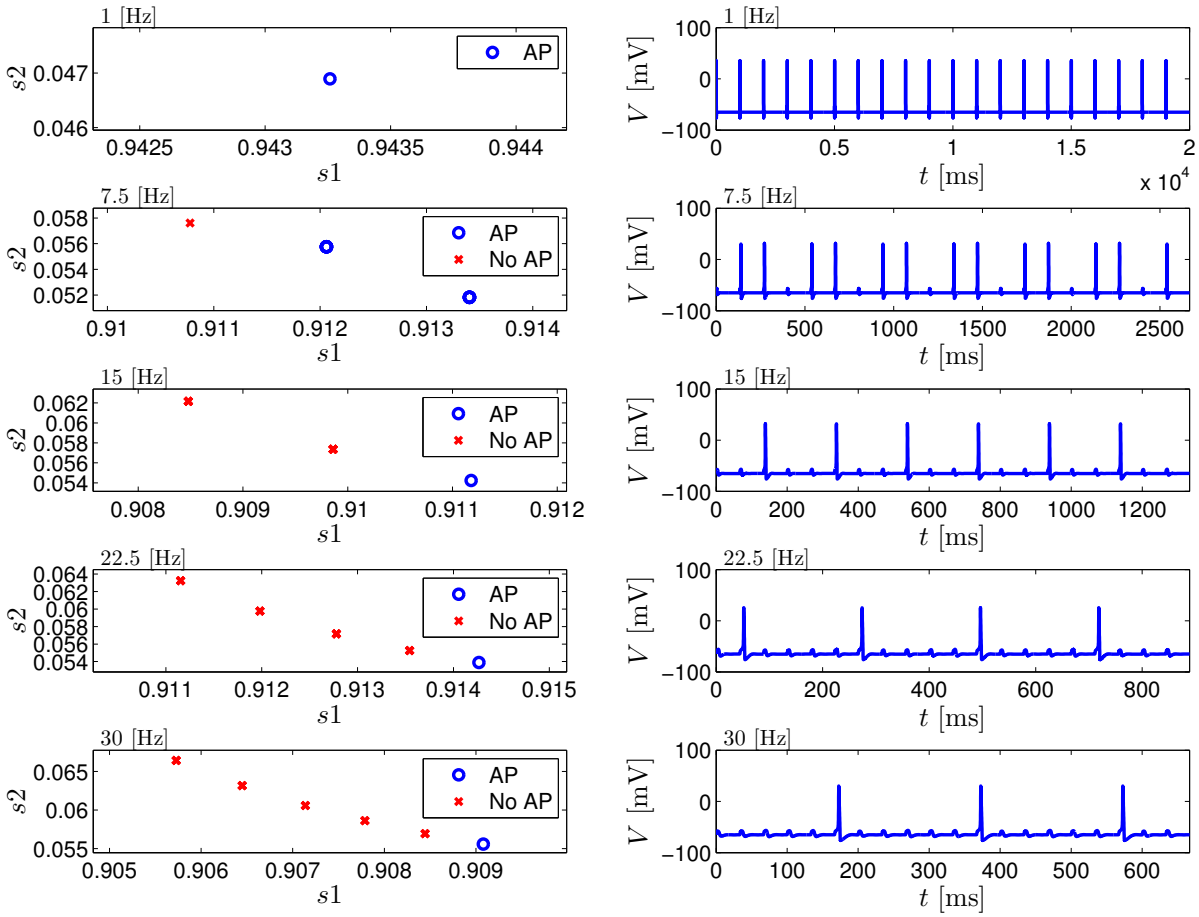

Figure 2: 1D firing patterns in 2D HHSAP model for different stimulation frequencies ($I_0 = 8.1\ \mu$A): **(Left)** During steady state, $\mathbf{w} \cdot \Delta\mathbf{s}^+ < 0$, therefore $\mathbf{s}$ lies on an approximately 1D limit cycle, which results in **(Right)** simple firing patterns (1:n or n:1) as in the 1D HHS model.

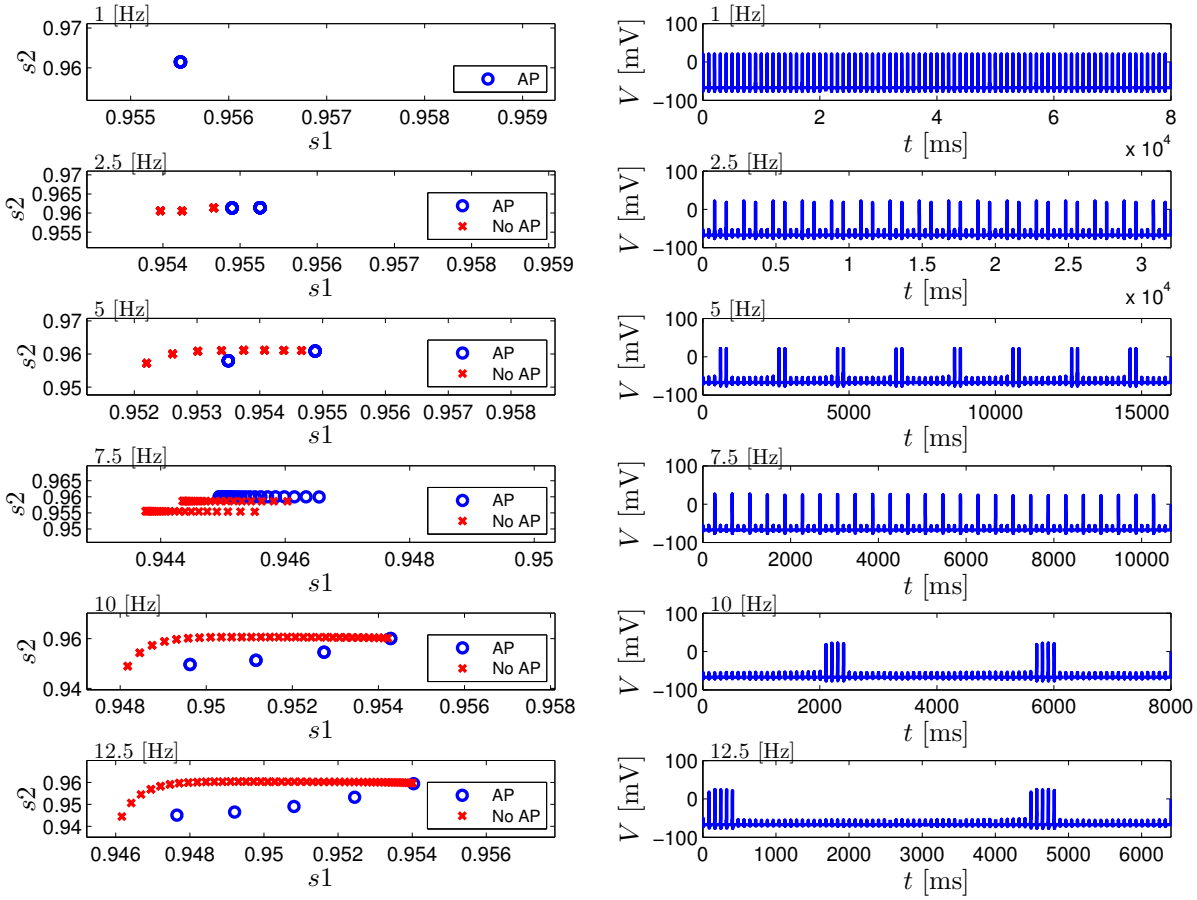

Figure 3: 2D HHSIP model ($I_0 = 13.3\ \mu$A): **(Left)** Steady limit cycles in $\mathbf{s}$ result in **(Right)** simple firing patterns. When $f_{\text{in}} = 5, 10$ or 12.5 Hz we get that $\mathbf{w} \cdot \Delta\mathbf{s}^+ > 0$ resulting in "bursts" (m:n firing patterns). When $f_{\text{in}} = 2.5$ or 7.5 Hz , $\mathbf{w} \cdot \Delta\mathbf{s}^- < 0$ and a simple 1D limit cycle is obtained. Note that for 7.5 Hz a steady state has not been completely reached yet, so the 1D limit cycle "drifts" to the left.

References

[1] W K Chandler and H Meves. Slow changes in membrane permeability and long-lasting action potentials in axons perfused with fluoride solutions. *The Journal of Physiology*, 211(3):707, 1970.

[2] P Dayan and L F Abbott. *Theoretical neuroscience: Computational and mathematical modeling of neural systems*. MIT Press, 2001.

[3] I A Fleidervish, A Friedman, and M J Gutnick. Slow inactivation of Na+ current and slow cumulative spike adaptation in mouse and guinea-pig neocortical neurones in slices. *J Physiol*, 493:83–97, 1996.

[4] A L Hodgkin and A F Huxley. A quantitative description of membrane current and its application to conduction and excitation in nerve. *The Journal of physiology*, 117(4):500, 1952.

[5] B Y B Rudy. Slow inactivation of the sodium conductance in squid giant axons. Pronase resistance., November 1978.

[6] M Yamada, C Koch, and P R Adams. *Multiple channels and calcium dynamics. In: Koch C, Segev I Methods in neuronal modeling.*, volume 484. MIT press, Cambridge, 1989.